Glass Transition of Microtome-Sliced Thin Films

Xiaorong Wang* and Wensheng Zhou

Bridgestone/Firestone Research Center, 1200 Firestone Parkway, Akron, Ohio 44317

Received February 21, 2002

The anomalous change of the glass transition temperature, T_g, of materials in confined geometry has drawn much attention recently.[1−20] The effective T_g in a thin film geometry, as measured by spectroscopic ellipsometry, X-ray reflectivity, and Brillouin scattering, can strongly depend on the film thickness as well as the polymer molecular weight.[2−6,8−13] Particularly, the measurement[9] of a free-standing polystyrene film has showed a 70 °C depression of the effective T_g for film thicknesses approaching several tens of nanometers. The physical origin of this change in T_g is so far unclear and has been the subject of much discussion. Various explanations have been proposed, including the decrease in film density,[14] the decrease in entanglement,[15] the enrichment of chain ends on surface,[16,17] and the enhancement of mobility on the surface layers.[7,9] De Gennes[18] has recently proposed that the polymer chain connectivity might play an important rule in this problem. The loops of polymer chains extended to the surface region of a thin film may allow a reptation-like dynamics, i.e., the loop sliding at the surface to penetrate from the surface inside the film, which results in a kinetically driven depression of T_g in thin films. However, there are several unresolved issues pertaining to the problem. First, all of the experimental results reported so far are based on study of spin-cast polymer films. It has been reported that the packing density of the spin-cast films is usually lower than bulk samples.[14,19,20] Second, the sliding dynamics is applicable only for linear polymers. As for branched polymers, this dynamics will largely be suppressed.[18] Third, the thermodynamic features of a polymer thin film are less discussed. Particularly, there is no report concerning the changes in the heat capacity, ΔC_p, of a thin polymer film from glass to liquid.

To understand the nature of this anomaly, we studied the glass transition behavior of a highly cross-linked polymer thin film. The polymer thin films were obtained by ultra-microtome slicing of a highly cross-linked bulk glass. Thus, the arguments concerning the difference in molecular packing density between thin films and bulk samples would not apply here. The glass transition of the thin films was measured using modulated differential scanning calorimetry (MDSC). We report our observations based on this study and briefly consider their implication on the kinetic concept of the depression of the effective T_g in polymer thin films.

The polymer glass used in this study was a fully cured epoxy resin. The liquid epoxy monomer used was diglycidyl ether of bisphenol A with an epoxide equivalent weight of 174.3 g/equiv. The amine-curing agent used was 4,4-methylene dianilene (MDA) with an amine equivalent weight of 49.5 g/equiv. Both chemicals were purchased from Aldrich. In preparation, a stoichiometric amount of the amine was dissolved into the liquid epoxy at approximately 80 °C. Complete dissolution took place within 30 min with vigorous stirring. Once the solution was clear, it was degassed under vacuum at 50 °C for 30 min. The degassed molten mixture was then filled into a multicavity silicon mold. The mold was then cured in an oven under nitrogen atmosphere at 140 °C for about 24 h and then at 200 °C for an additional 12 h.

The cross-linking density, X_d, of the material was estimated via the equation[21] $X_d = \rho[\omega_1(a - 2)/M_1 + \omega_2(b - 2)/M_2]N_{av}$, where ρ is the density of the material, ω_1 is the weight fraction of the epoxy monomer, ω_2 is the weight fraction of the amine monomer, M_1 is the molecular weight of the epoxy monomer, M_2 is the molecular weight of the amine monomer, a is the functionality of the epoxy monomer, b is the functionality of the amine monomer, and N_{av} is Avogadro's number. The mean distance between two cross-linking sites, l, can be estimated from the relation $l \sim X_d^{-1/3}$. For the epoxy resin employed in this research, the functionality of the diglycidyl ether of bisphenol A is 2, and the functionality of the 4,4-methylenedianilene is 4. If the material is fully cured and the density is $\rho = 1.22$ g/cm^3, the cross-linking density will be $X_d \sim 1.7$ site/nm^3 and the mean distance between two cross-linking sites will be $l \sim 0.84$ nm or 8.4 Å.

The thin films were sliced from the fully cured epoxy polymer glass using a Leica Emfcs Ultracut UCT Ultramicrotome equipped with a diamond knife at 40 mm/s cutting rate. The block face for the sample preparation was about 2 × 2 mm. The slicing was processed at 23 °C, and the sliced sections were floated off onto water in the conventional fashion of room temperature ultramicrotomy.[22] Two knives were used and alternately cleaned after a couple hundred cuts. The quality of sections was generally monitored by a recording camera. Sections of a nominal 40 nm thickness were collected first. The process was then repeated to collect sections of 80 nm thickness and then 120 nm. During slicing, a random sampling of sections were collected on a mica surface and examined on a Digital Instrument Dimension 3000 atomic force microscope (AFM) in tapping mode with etched silicon tips (Nanoprobe). Under the microscope, the sections appeared to be in accordion-type folding shape (see Figure 1). The accordion-type crumpling was caused by the high-speed cutting rate. The distance between two adjacent folds for the film shown in Figure 1 was about 2 μm, and the height between the base and the top of the fold (or the ridge) was about 0.2 μm. The thickness of the film, depending on the microtome setup, could be estimated by measuring the height between the mica surface and the film at the nearest valley points. The thickness distribution, as shown in Figure 1, was taken from a number of randomly selected films. The reported thickness for each group of films in Table 1 was the average of the measurements. The error listed was the standard variation σ_{n-1}. For a single film, the roughness could also be estimated by breaking one accordion-folded film into many small pieces and then taking the measurement when they laid down on the mica surface. The standard variation for the thickness of a single film was not included in the calculation and was usually smaller than the standard variation for a group of the films. For DSC measurements, the sections were picked up using

10.1021/ma020291r CCC: $22.00
Published on Web 08/03/2002

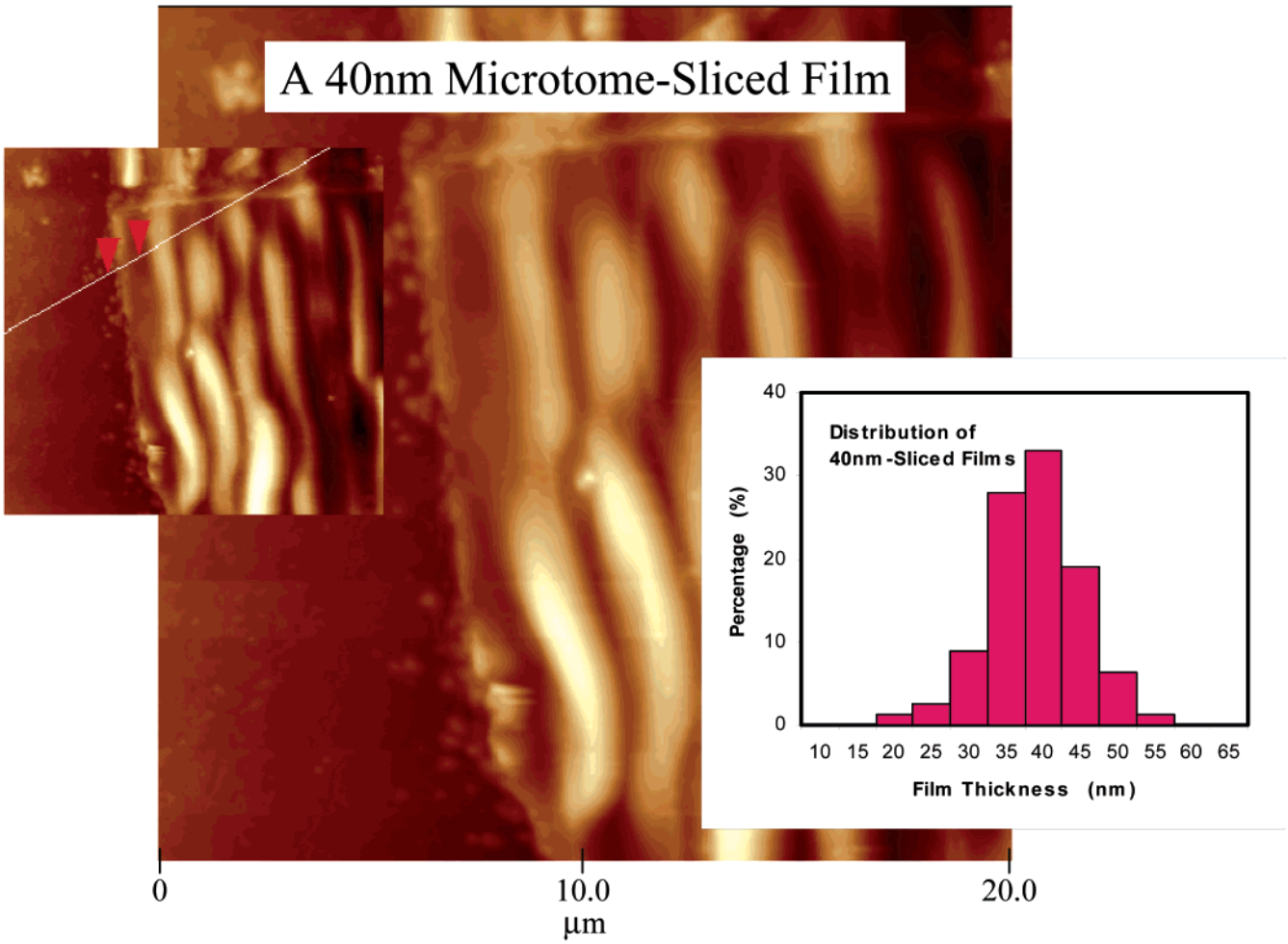

Figure 1. Atomic force microscopy picture of a 40 nm microtome-sliced thin film. The inset on the left shows the measurement of the thickness of the film. Arrows marks the locations of mica surface and the film surface where the measurement is taken. The thickness is about 37 nm for the film. The inset on the right shows the thickness distribution for a number of randomly selected films. The standard variation σ_{n-1} was about 6.3 nm.

Table 1. Effect of Film Thickness on T_g and ΔC_p

film thickness (nm)	midpoint T_g (°C)	onset T_g (°C)	ΔC_p (J/g/°C)	midpoint $C_{p,\text{mid.}}$	max T_s (°C)	coperative size ξ (nm)
38.9 ± 6.3	167.4	154.3	0.246	2.93	70	16.9
	163.9	149.1	0.232	3.14	75	15.1
80.3 ± 10.1	175.1	170.6	0.220	3.03	95	23.0
	175.1	163.2	0.231	2.98	100	17.1
	173.6	163.4	0.245	2.97	102	18.3
121.4 ± 13.4	179.4	167.9	0.257	2.89	150	18.4
	178.2	166.9	0.236	2.87	140	18.0
bulk	179.4	170.1	0.230	3.19	n/a	17.8
	179.8	170.5	0.245	2.95	n/a	19.1

a small glass plate and then carefully scrapped onto a watch glass. This cutting/collecting process was relatively straightforward, though it might take several days to obtain about 1 mg of thin films. The films were finally dried under vacuum at 50 °C for about a week and then kept in freezer until use. Visually, those films looked like highly porous fine powders.

Thermal analysis was performed on a TA instrument modulated DSC 2920 using a nitrogen-purged cell at a flow rate of 60 mL/min. The heat capacity signal was calibrated using a sapphire at 5 °C/min, 40 s period, and 0.5 °C modulating amplitude. Thin films of about 1−2 mg were carefully weighed into a DSC aluminum pan and then encapsulated and crimped. The variables measured were the total heat flow, reversible heat flow, nonreversible heat flow, and heat capacity. The glass transition temperature, T_g, was determined from the heat capacity vs temperature profile. Prior to the measurement, all samples were further annealed at 200 °C and were then cooled to room temperature at a constant rate of 5 °C/min. This procedure resulted in samples with well-defined and reproducible thermal history. It should be noted that the annealing did not cause these thin films to melt together because they were highly cross-linked.

The heat capacity C_p for various samples is plotted vs temperature in Figure 2. The discontinuous behavior of the heat capacity at the glass transition is virtually the same for both film and bulk samples. Table 1 lists the step changes in the heat capacity, ΔC_p, at the glassy transition for film thickness from 40 to 120 nm. The transition-induced ΔC_p is not sensitive to the film thickness. This observation agrees with that reported by Jackson and McKenna for small organic molecules

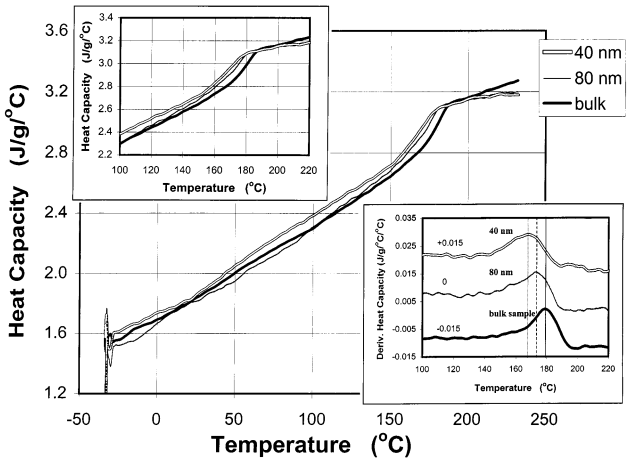

Figure 2. Heat capacity vs temperature for various samples. The inset on the left shows the details of the glass transition region. The inset on the right shows the breath of the glass transition.

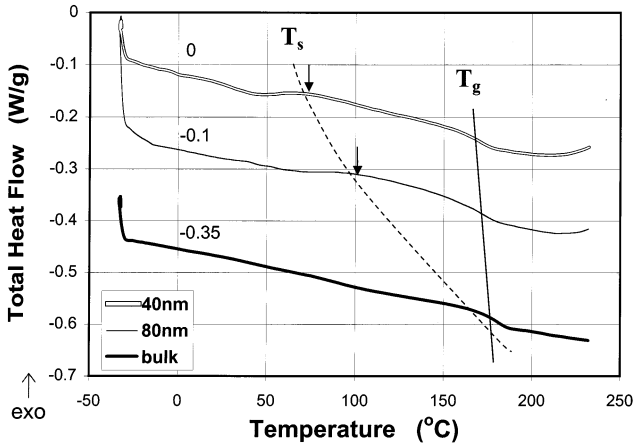

Figure 3. Total heat flow vs temperature for various samples. Two events appear in the thermal diagram: the distortion peak at T_s and the glass transition at T_g.

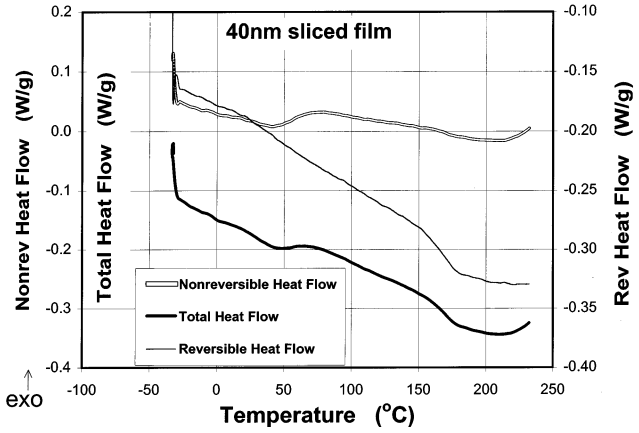

Figure 4. MDSC diagram for 40 nm microtome-sliced films. The variables measured are the total heat flow, reversible heat flow, and nonreversible heat flow.

confined in nano pores,[1,23,24] but it is not in agreement with the results reported by Hempel et al. for benzoin isobutyl ether[25] in the same conditions. The breadth of the glass transition for the microtome-sliced films increases slightly with decreasing the film thickness; however, the change is not as dramatic as that reported for spin-cast thin films.[11] For convenience, the onset and midpoint values of the T_g for films with thickness from 40 to 120 nm are also listed in Table 1.

The measured value of glass transition temperature T_g depends on the film thickness. As shown in Figure 2, the thinner the film, the lower the T_g. Comparing to bulk samples, a 15 °C reduction of T_g is observed for films with thickness of 40 nm. This phenomenon is completely reproducible if one runs the same sample pan twice. The reason is that the highly cross-linked films stay intact and do not flow together during the heating cycle. The reduction of T_g in the microtome-sliced films is similar in direction, but smaller in magnitude than the reduction reported in spin-cast thin films. For example, a 70 °C depression in T_g was reported for spin-cast polystyrene thin films.[8,9] In our study, it also appears that at 120 nm thickness the thin film behaves like a bulk sample.

However, there are some stunning features of the microtome-sliced thin films deep in the glassy state. Figure 3 shows the change of total heat flow vs temperature for various samples. The microtome-sliced thin films display a broad exothermic distortion peak deep in the glassy state. This distortion peak starts at a temperature somewhere far below T_g and ends when the glass transition is encountered. The maximum of the peak strongly depends on the film thickness. Its location (T_s) decreases dramatically as the film thickness decreases. The same distortion peak, however, is not observed for bulk samples. An important fact is that this distortion peak exists in the total heat flow signal and the nonreversible heat flow signal, but not in the reversible heat flow and C_p signals (see Figure 4). Hence, the phenomenon is a kinetically driven event.

The effect of the finite size on the glass transition as described above cannot be interpreted in terms of proposed kinetic theories.[7,9,14−18] First, the packing density (or the free volume fraction) should be the same for both films and bulk samples, since the films examined here were directly cut from the bulk glass. Second, it is unlikely that the change in entanglements would explain this effect, since the polymer glass is highly cross-linked. Third, the reptation-like dynamics[18] would not be sufficient to provide a penetration of surface motions deep into the film, because the branched polymer structure will largely suppress the dynamics and make it become impossible in the highly cross-linked state. We realize that microtome-slicing may damage cross-linkages and thus could cause the observed decrease in T_g. However, our analysis has shown that the mean distance (l) between two cross-linked sites is about 1 nm, making it unlikely that the damage induced by slicing process is responsible for the 15 °C shift of T_g in films of thickness of 40 nm. One may argue that the molecular motion near the glass transition adopts a cooperative nature.[26] The probability of a cooperative rearrangement is a function of the cooperative size ξ, which increases as the temperature decreases.[26] Therefore, the reduction of T_g in the thin films can be viewed from the physical picture of a confined cooperative rearrangement.[25] However, at the glass transition, the value of the cooperative size, ξ, can be estimated from the available DSC data[27] via $\xi \cong (k_B T_g^2 \Delta C_p / C_{p,\mathrm{mid}} \rho \delta T^2)^{1/3}$, where δT is the breath of the glass transition and $C_{p,\mathrm{mid}}$ is the middle point at the transition between glass and liquid. Table 1 lists the calculated cooperative size ξ for thickness from 40 to 120 nm. The value of ξ for thin films closely equals the bulk value. Under these circumstances, it would be

reasonable to compare[23] the glass transition to second-order transitions such as those predicted by Ising models.[28,29] The effect of finite size would shift the T_g temperature downward because in Ising models the critical temperature in the two dimensions is lower than its corresponding value in three dimensions.

The discovery of a broad distortion peak deep in the glassy state for thin films is surprising. The interesting fact is that the distortion peak is reproducible and shifts downward dramatically with the decrease of the film thickness. We do not know the reason yet but speculate that the phenomenon may be due to the internal stresses that have been frozen during cross-linking reactions (or cure). In the gelled state during cure, stresses can be inevitablely generated. Our reasoning originates from the observation of such distortion peaks in many polymer fibers, where polymer chains are stretched in the fiber formation process.

In summary, the glass transition behavior of a highly cross-linked polymer thin film was studied by modulated differential scanning calorimetry (MDSC). The polymer thin film was obtained by microtome slicing of a bulk glass at room temperature. Compared to the case of bulk samples, a reduction of 15 °C in T_g was observed for film thickness of 40 nm. This reduction in T_g is similar in direction, but smaller in magnitude than the reduction reported in spin-cast films. Deep in the glassy state, these microtome-sliced films also showed an anomalous broad exothermic peak. The location of the peak was observed to decrease with decreasing film thickness. The change in heat capacity, ΔC_p, at the glass transition for thin films, however, was found to match with the bulk samples. These observations on highly cross-linked films cannot be explained adequately by proposed kinetic theories.

Acknowledgment. We thank P. Sadhukhan for the use of his microscopy laboratory. B. M. Cernik is gratefully acknowledged for his help on microtome slicing.

References and Notes

(1) Jackson, C. L.; Mckenna, G. B. *J. Chem. Phys.* **1990**, *93*, 9002.
(2) Beaucage, G.; Composto, R.; Stein, E. S. *J. Polym. Sci., Part B: Polym. Phys.* **1993**, *31*, 319.
(3) Orts, W. J.; van Zanten, J. H.; Wu, W. L.; Satija, S. K. *Phys. Rev. Lett.* **1993**, *71*, 867.
(4) van Zanten, J. H.; Wallace, W. E.; Wu, W. L. *Phys. Rev. E* **1996**, *53*, r2053.
(5) Wallace, W. E.; van Zanten, J. H.; Wu, W. L. *Phys. Rev. E* **1995**, *52*, r3329.
(6) Wu, W. L.; van Zanten, J. H.; Orts, W. J. *Macromolecules* **1995**, *28*, 771.
(7) Arndt, M.; Stannarius, R.; Groothues, H.; Hempel, E.; Kremer, F. *Phys. Rev. Lett.* **1997**, *79*, 2077.
(8) Keddie, J. L.; Jones, R. A. L.; Cory, R. A. *Europhys. Lett.* **1994**, *27*, 59.
(9) Forrest, J. A.; Dalnoki-Veress, K.; Stevens, J. R.; Dutcher, J. R. *Phys. Rev. Lett.* **1996**, *77*, 2002.
(10) Deppe, D. D.; Dhinojwala, A.; Torkelson, J. M. *Macromolecules* **1996**, *29*, 3898.
(11) Hall, D. B.; Hooker, J. C.; Torkelson, J. M. *Macromolecules* **1997**, *30*, 667.
(12) Fryer, D. S.; Nealey, P. F.; de Pablo, J. J. *Macromolecules* **2000**, *33*, 6439.
(13) Kerle, T.; Lin, Z.; Kim, H. C.; Russell, T. P. *Macromolecules* **2001**, *34*, 3484.
(14) Reiter, G. *Macromolecules* **1994**, *27*, 3046.
(15) Brown, H. R.; Russell, T. P. *Macromolecules* **1996**, *29*, 798.
(16) Tanaka, K.; Taura, A.; Ge, S. R.; Takahara, A.; Kajiyama, T. *Macromolecules* **1996**, *29*, 3040.
(17) Kajiyama, T.; Tanaka, K.; Takahara, A. *Macromolecules* **1997**, *30*, 280.
(18) de Gennes, P. G. *Eur. Phys. J.* **2000**, *E2*, 201.
(19) DeMaggio, G. B.; Frieze, W. E.; Gidley, D. W.; Zhu, M.; Hristov, H. A.; Yee, A. F. *Phys. Rev. Lett.* **1997**, *78*, 1524.
(20) Jean, Y. C.; Zhang, R.; Cao, H.; Yuan, J. P.; Hang, C. M.; Nielsen, B.; Asoka-Kumar, P. *Phys. Rev. B* **1997**, *56*, r8459.
(21) Wang, X. *J. Appl. Polym. Sci.* **1997**, *64*, 69.
(22) Ruokolainen, J.; Tanner, J.; Ikkala, O.; ten Brinke, G.; Thomas, E. L. *Macromolecules* **1998**, *31*, 3532. In the summer of 1999, Ruokolainen also made a visit to our research center in Akron and showed us how to microtome slice thin films at room temperature.
(23) Jackson, C. L.; Mckenna, G. B. *J. Non-Cryst. Solids* **1991**, *131*, 221.
(24) Jackson, C. L.; Mckenna, G. B. *Chem. Mater.* **1996**, *8*, 2128.
(25) Hempel, E.; Huwe, A.; Otto, K.; Janowski, F.; Schroter, K.; Donth, E. *Thermochim. Acta* **1999**, *337*, 163.
(26) Adam, G.; Gibbs, J. H. *J. Chem. Phys.* **1965**, *43*, 139.
(27) Donth, E. *J. Polym. Sci., Part B: Polym. Phys.* **1996**, *34*, 2881.
(28) Douglas, J. F.; Ishinable, T. *Phys. Rev. E* **1995**, *51*, 1791.
(29) Sappelt, D.; Jackle, J. *J. Phys. A* **1993**, *26*, 7325.

MA020291R